Geochronology and Geochemistry of Early Cretaceous Granitic Rocks in the Dongqiao Area, Central Tibet: Implications for Magmatic Origin and Geological Evolution

Hao Wu,[1,2,3,*] *Zhaxi Qiangba,*[3] *Cai Li,*[4] *Qiang Wang,*[2,5] *Wangdui Gesang,*[3] *Ouzhu Ciren,*[3] *and Dunzhu Basang*[3]

1. School of Earth Sciences and Engineering, Hohai University, Nanjing 210098, China; 2. State Key Laboratory of Isotope Geochemistry, Guangzhou Institute of Geochemistry, Chinese Academy of Sciences, Guangzhou 510640, China; 3. Regional Geological Survey Party, Tibet Bureau of Geology and Mineral Exploration and Development, Doilungdegen 851400, China; 4. College of Earth Sciences, Jilin University, Changchun 130061, China; 5. CAS Center for Excellence in Tibetan Plateau Earth Sciences, Beijing 100101, China; and University of Chinese Academy of Sciences, Beijing 100049, China

ABSTRACT

We present here new geochronological and whole-rock geochemical data for the Dongqiao intrusive rocks. Six samples yield zircon U-Pb ages of 111–115 Ma, indicating that the Dongqiao granitic rocks are contemporaneous with an Early Cretaceous (115–110 Ma) magmatic flare-up event in central Tibet. On the basis of geochemical data, granitic rocks from the Dongqiao area can be divided into I- and A-type granites. The A-type granites contain higher $Na_2O + K_2O$, Zr, Hf, and Zr + Ce + Nb + Y contents than the I-type granites. The results indicate that I-type granites were formed by partial melting of a juvenile mafic lower-crustal source, while A-type granites were derived from a middle-crustal source, followed by fractional crystallization. The formation of A-type granites requires broad thermal anomalies, indicating that Early Cretaceous magmatism occurred in a postcollision extensional setting, likely related to the upwelling of hot asthenospheric mantle triggered by detachment and sinking of the Bangong-Nujiang oceanic lithosphere.

Online enhancements: supplemental tables.

Introduction

The tectonic evolution of continent-continent collision zones involves a cycle of oceanic opening and closing followed by collision of continents, continental fragments, slab breakoff, crustal thickening, and subsequent lithospheric delamination (cf. Lustrino 2005). Although it is generally agreed that the Tibetan Plateau was formed by a sequence of oceanic subduction and continental collision processes (e.g., Dewey et al. 1988; Yin and Harrison 2000; Ding et al. 2003; Chung et al. 2005; Pan et al. 2012; Wu et al. 2016*a*, 2016*b*), the details of its evolution are still widely debated (e.g., Pan et al. 2012; Zhu et al. 2013, 2016).

Manuscript received March 27, 2017; accepted September 14, 2017; electronically published January 18, 2018.

* Author for correspondence; e-mail: wuhaojlu@126.com.

Collision of the Lhasa and Qiangtang terranes, which occurred during closure of the Bangong-Nujiang Ocean (now represented by the Bangong-Nujiang suture zone [BNSZ]; fig. 1*a*, 1*b*), was an important phase in the geologic evolution of the Tibetan plateau (Dewey et al. 1988; Yin and Harrison 2000; Kapp et al. 2005, 2007; Leier et al. 2007*a*, 2007*b*). However, details of the evolution of the Bangong-Nujiang Ocean remain debated, including the Early Cretaceous tectonic setting of central Tibet. Some workers suggested that the Early Cretaceous magmatism formed during the subduction of the Bangong-Nujiang Ocean lithosphere, such as the slab rollback or northward subduction of the ocean ridge (Wu et al. 2015*a*; Xu et al. 2017). Others believed that the magmatism erupted under a postcollisional extensional environment, which were most likely triggered by slab breakoff associated with the south-

[The Journal of Geology, 2018, volume 126, p. 249–260] 0022-1376/2018/12602-0006$15.00. DOI: 10.1086/695702

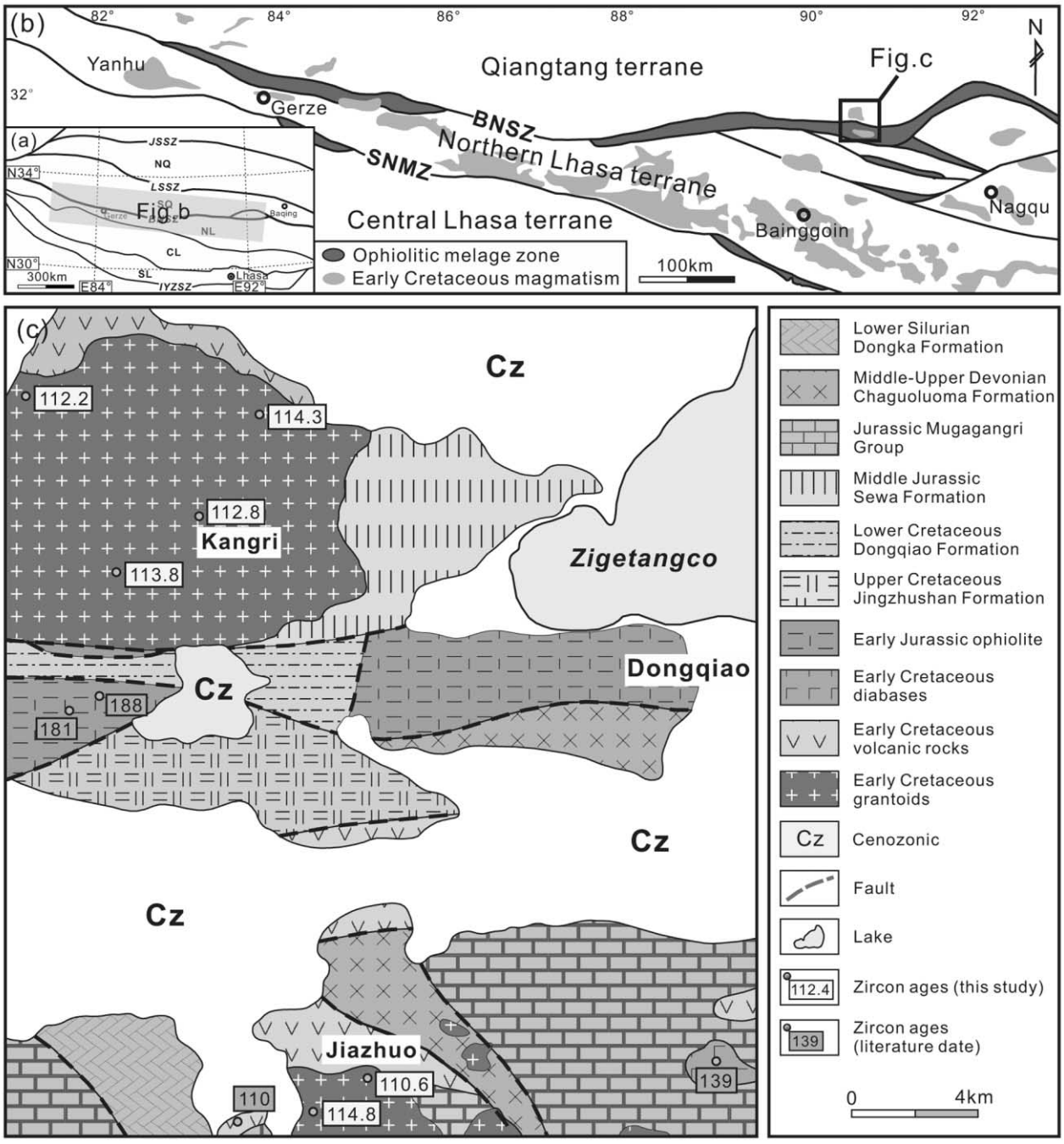

Figure 1. Geographical and geological setting of the Dongqiao area. *a*, Simplified geological map of the Tibetan Plateau showing the major blocks (ovals with numerals). *b*, Simplified geological map showing the Early Cretaceous magmatism in the Lhasa-Qiangtang collision zone (Zhu et al. 2009). *c*, Geological map of the Dongqiao area. Abbreviations: JSSZ = Jinsha Suture Zone; BNSZ = Bangong-Nujiang Suture Zone; SNMZ = Shiquan River–NamTso Mélange Zone; IYZSZ = Indus–Yarlung Zangbo Suture Zone; NQ = Northern Qiangtang terrane; SQ = Southern Qiangtang terrane; NL = Northern Lhasa subterrane; CL = Central Lhasa subterrane; SL = Southern Lhasa subterrane. Age data sources: Liu et al. 2015; Qiangba et al. 2016.

ward subduction of the ocean lithosphere or detachment of the ocean lithosphere after the bidirectional subduction (e.g., Zhu et al. 2009, 2011, 2016; Sui et al. 2013; Wu et al. 2015*b*).

Characteristics of large-scale Early Cretaceous magmatism recorded on both sides of the BNSZ may help to resolve these controversies. To further understand the evolution of the Bangong-Nujiang

continent-continent collision zone and to constrain the petrogenesis and tectonic setting of the Early Cretaceous magmatic rocks, we conducted detailed geological fieldwork and sampling in the Dongqiao area. Here we present new geochronological and whole-rock geochemical data for the Early Cretaceous granitic rocks of the Dongqiao area. These new data—in combination with our field observations and other recent research on the central Tibet—provide important new insights into magmatic processes operating in continent-continent collision zones in Tibet and worldwide.

Geological Background and Field Observations

The Tibetan Plateau, from north to south, consists of the Kunlun-Qaidam and Songpan-Ganze blocks, northern Qiangtang terrane, southern Qiangtang terrane, Lhasa terrane, and Himalaya terrane. These terranes are separated by a series of suture zones, termed Jinsha, Longmu Tso–Shuanghu, Bangong-Nujiang, and Indus–Yarlung Zangbo suture zones. On the basis of the distribution of various sedimentary units and ophiolite sequences, the Lhasa terrane can be further divided into northern, central, and southern subterranes, with the Shiquan River–Nam Tso Mélange Zone separating the northern and central subterranes and the Luobadui–Milashan Fault separating the central and southern subterranes (Zhu et al. 2011; fig. 1*a*).

The Dongqiao area is located on the southern margin of the southern Qiangtang terrane, central Tibet (fig. 1*b*). The regional tectonic evolution of this area was primarily affected by the evolution of the Bangong-Nujiang Ocean lithosphere in the Mesozoic. Stratigraphic units in the study area are complex and diverse. Magmatic rocks are widely distributed in the Dongqiao area and include Early Jurassic ophiolites and Early Cretaceous intrusive and volcanic rocks (fig. 1*c*). The Dongqiao intrusives are typically composed of monzonitic granite, granodiorites, and granites (fig. 2*a*, 2*b*). These intrusive rocks are in intrusive contact with surrounding limestone and sandstone units of Devonian and Jurassic strata and also unconformably overlain by Cenozoic sedimentary rocks.

For this study, we collected samples of Early Cretaceous intrusive rocks from extensive exposures in the Dongqiao area to constrain the age and geochemical nature of these rocks. Six samples were selected for zircon U-Pb dating, and 45 samples were collected for geochemical analyses. The samples were generally fresh and with different petrographic characteristics. The granodiorites have a porphyritic texture and consist primarily of quartz (25 vol%),

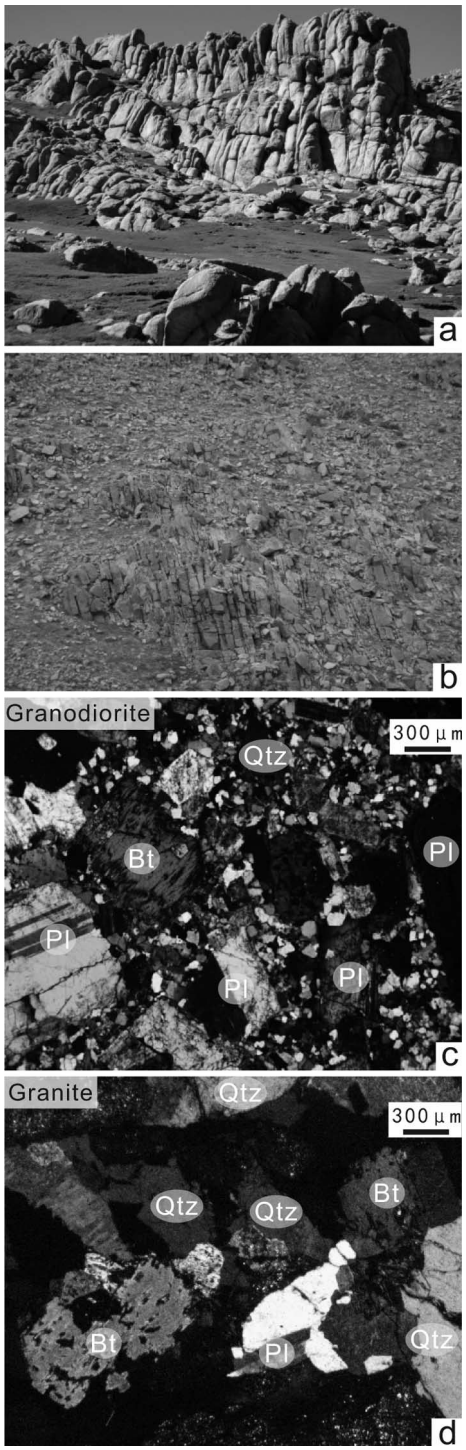

Figure 2. Photomicrographs of the Dongqiao granitic rocks (cross-polarized light). *a*, *b*, Close-up photograph of the intrusive rocks. *c*, *d*, Photomicrographs (cross-polarized light) showing the textures of granodiorites and granites. Abbreviations: Qtz = quartz; Pl = plagioclase; Bt = biotite.

plagioclase (25 vol%), K-feldspar (10 vol%), biotite (5 vol%), and amphibole (15 vol%; fig. 2*c*). The granites are fine grained and have a mineral assemblage of quartz (55 vol%), zoned plagioclase (20 vol%), and biotite (15 vol%), with accessory zircon, apatite, and Fe-Ti oxides (fig. 2*d*).

Age Constraints

U-Pb Zircon Geochronological Data. Six intrusive rock samples were collected for zircon U-Pb age dating using laser ablation inductively coupled plasma mass spectrometry. Descriptions of the analytical methods used in the study are given in the appendix, and the results are listed in table S1 (tables S1 and S2 are available online).

All of the zircons from granitic rocks (samples TW38221, TW38222, 11DGQ, PM00114, PM00120, and PM0086) have relatively high Th/U ratios of 0.49–1.72 (i.e., >0.1). Calculated $^{206}Pb/^{238}U$ ages of 111–121 Ma (TW38221), 107–115 Ma (TW38222), 111–121 Ma (11DGQ), 109–118 Ma (PM00114), 110–118 Ma (PM00120), and 107–116 Ma (PM0086) are nearly concordant, with weighted-mean ages of 114.7 ± 1.0 Ma (n = 28; MSWD = 8.8; fig. 3*a*), 110.5 ± 1.1 Ma (n = 20; MSWD = 11; fig. 3*b*), 114.5 ± 1.7 Ma (n = 17; MSWD = 12; fig. 3*c*), 113.1 ± 1.0 Ma (n = 23; MSWD = 7.8; fig. 3*d*), 114.0 ± 0.8 Ma (n = 24; MSWD = 4.7; fig. 3*e*), and 112.4 ± 0.9 Ma (n = 20; MSWD = 5.5; fig. 3*f*), respectively.

Age around Dongqiao Area. Our new results show that the granitic rocks from the Dongqiao area can be dated to 115–111 Ma. This date is also coeval with the ages of magmatic rocks that have been studied along both sides of the BNSZ, including the Xainza volcanic rocks (111–114 Ma: Zhu et al. 2011; ca. 114 Ma: Kang et al. 2008; ca. 116 Ma: Chen et al. 2014), the Xainza host granodiorite and mafic enclaves (111–113 Ma: Zhu et al. 2009; Zhang et al. 2011), the Daguo volcanic rocks (ca. 116 Ma: Kang et al. 2009; ca. 114 Ma: Zhu et al. 2011), the Xainza A2-type granites (ca. 112 Ma: Qu et al. 2012), the Yanhu bimodal volcanic rocks (ca. 112 Ma: Sui et al. 2013), the Dachagou adakitic granodiorite (ca. 117 Ma: Wu et al. 2015*a*), and the Renaco bimodal volcanic rocks (ca. 110 Ma: Chang 2012). Those age data indicate that an extensive magmatic event erupted at 115–110 Ma, with significant compositional diversity around the Dongqiao area in central Tibet (fig. 1*b*).

Geochemical Composition and Classification

Geochemistry. Whole-rock major and trace element analyses were collected from 45 samples from the Dongqiao area. The descriptions of the analytical methods used are given in the appendix, and the results are listed in table S2.

Both petrographic observations and the range in loss on ignition values (0.53–3.08 wt%) indicate that all of the samples from the Dongqiao area have undergone weak alteration. The samples from the Dongqiao are characterized by high SiO_2 content and are classed as granitic rocks. These granitic samples are characterized by variable SiO_2 (62.2–74.2 wt%), Al_2O_3 (10.5–16.6 wt%), K_2O (2.33–5.07 wt%), Na_2O (2.23–4.70 wt%), and MgO (0.35–4.50 wt%). Mg number values are 25–57, and FeO^*/MgO ratios are 1.61–6.45. On the basis of the total alkali-silica classification diagram (Middlemost 1994), the granitic rocks can be classified as granodiorites, quartz

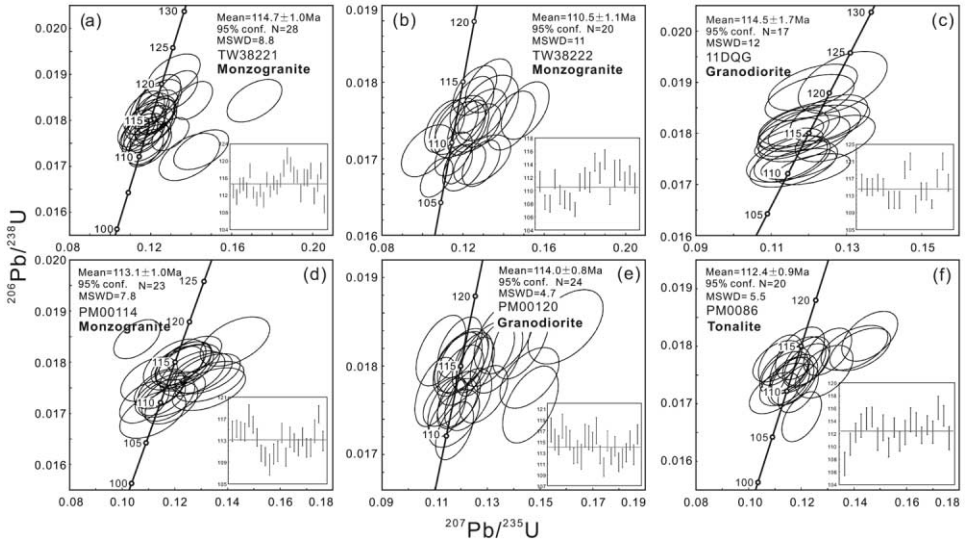

Figure 3. U-Pb concordia diagrams of zircons from Dongqiao granitic rocks.

monzonites, and granites (fig. 4*a*). All the samples exhibit high potassium contents, which is a feature of high-K calc-alkaline series rocks (fig. 4*b*). In addition, all samples show high-K calc-alkaline and shoshonite series characteristics on the Th versus Co plot (fig. 4*c*; Hastie et al. 2007). On the A/NK versus A/CNK diagram, most of these granitic rocks show metaluminous to slightly peraluminous features with A/CNK ratios of 0.88–1.08, except one sample with A/CNK ratios of 1.22 (fig. 4*d*; Maniar and Piccoli 1989).

Whole-rock analyses of the granitic rocks yield chondrite-normalized rare earth element (REE) patterns (fig. 5*a*) and show that the rocks are enriched in light REEs ($(La/Yb)_N$ = 6.32–23.6) and contain moderately negative Eu anomalies (Eu/Eu^* = 0.54–1.01). When plotted on a primitive mantle–normalized variation diagram (fig. 5*b*), samples are enriched in large ion lithophile elements (e.g., Rb, Th) and depleted in high field strength elements (e.g., Nb, Ta).

Classification. As mentioned above, samples from the Dongqiao area exhibit variable concentrations of major and trace elements (fig. 6). The widely used granite classification scheme of Chappell and White (1974) subdivides granites into I-, S-, A- and M-type, according to magma source and tectonic setting. The granitic samples have relatively low A/CNK ratios (fig. 4*d*) with few or no Al-rich minerals (e.g., cordierite or muscovite), indicating that the samples do not possess the characteristics of S-type granites. According to the Zr + Ce + Nb + Y contents, the granitic sample could be divided into two groups (fig. 7*a*, 7*b*). The samples (n = 27) with low Zr + Ce + Nb + Y contents (<350 ppm) show increases in Th and Y with increasing Rb, which is typical of I-type granite (fig. 7*a*, 7*b*). Hence, we suggest that the most samples from the Dongqiao area are normal calc-alkaline I-type granitoids (Whalen et al. 1987; Chappell 1999).

However, the samples (n = 18) with high Zr + Ce + Nb + Y contents (>350 ppm) from the Dongqiao area are characterized by high contents of Na_2O + K_2O, Zr, and Hf (fig. 4*a*), which distinguishes them from normal I-type granites and makes them similar to typical A-type granites (Whalen et al. 1987; Watson et al. 2006). This similarity is further supported by relatively high zircon saturation temperatures of 792°–878°C (fig. 7*b*; table S2). Hence, we propose that the granitic samples from the Dongqiao area can be classified as both I- and A-type granites on the basis of their major and trace elements.

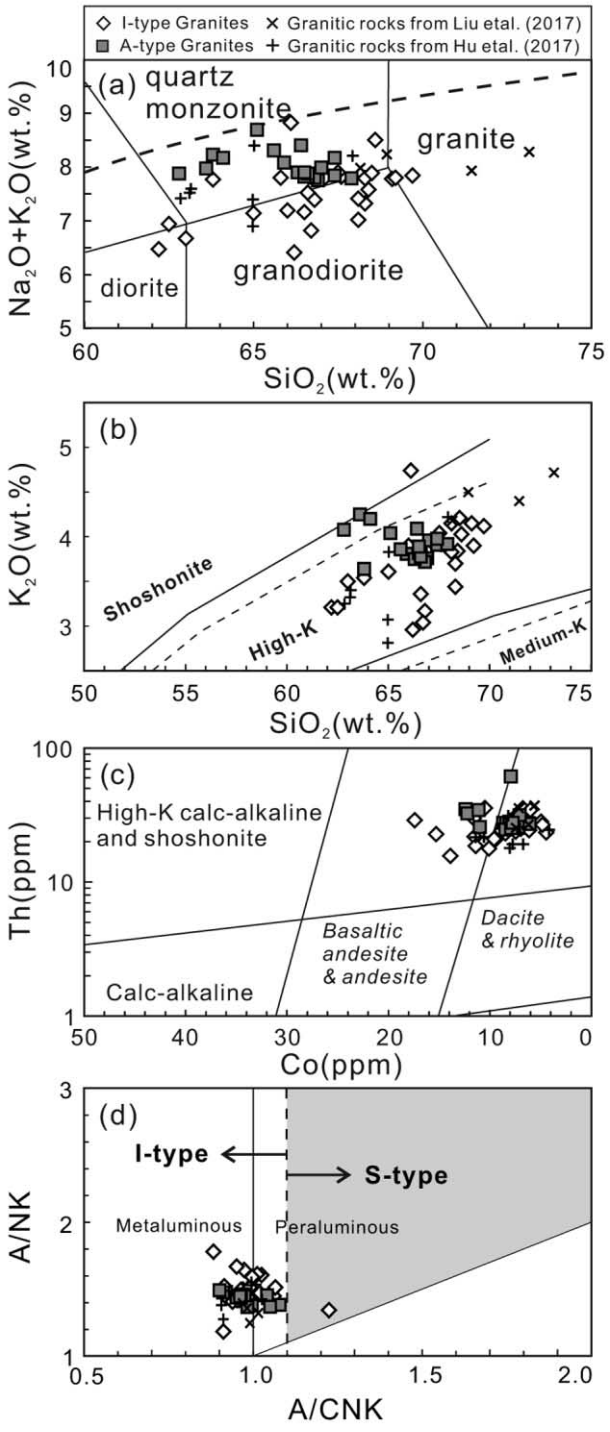

Figure 4. Geochemical classification of whole-rock samples of Dongqiao granitic rocks. *a*, Total alkali ($Na_2O + K_2O$) versus SiO_2 (Middlemost 1994). *b*, K_2O versus SiO_2 (Le Maitre et al. 1989; Rickwood 1989). *c*, Th versus Co (Hastie et al. 2007). *d*, A/NK versus A/CNK (Shand 1943).

Petrogenesis

I-Type Granites. Calc-alkaline I-type granites are generally considered to form by partial melting of

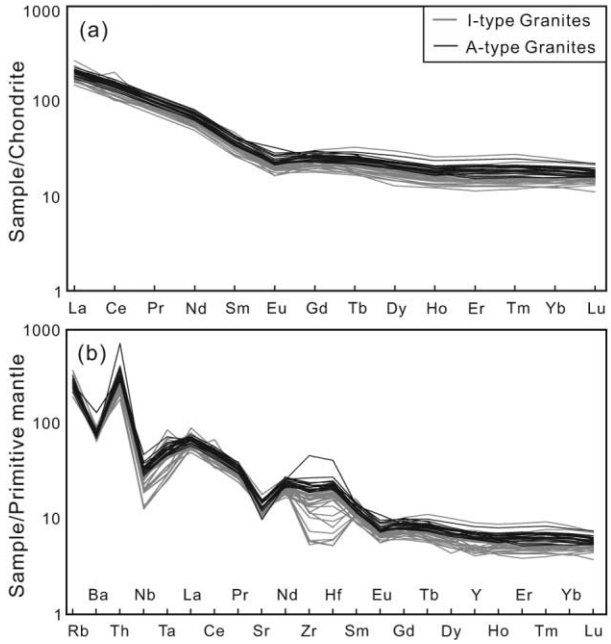

Figure 5. Chondrite-normalized rare earth element (*a*) and primitive mantle–normalized multielement (*b*) patterns (Sun and McDonough 1989) for Dongqiao granitic rocks.

mafic-intermediate metaigneous lower crust (Petford and Atherton 1996; Chappell 1999). Our I-type samples typically plot in the field of amphibolite experimental melts in an $Al_2O_3/(FeO_t + MgO + TiO_2)$ versus $Al_2O_3 + FeO_t + MgO + TiO_2$ diagram (fig. 8). Experimental studies show that dehydration melting of low-K basaltic rocks can produce intermediate-silicic melts that are typically low in K, have Na_2O/K_2O ratios of >1, have low contents of heavy REEs, and are high-Al trondhjemitic in composition (Rushmer 1991; Rapp and Watson 1995; Petford and Atherton 1996). In contrast, dehydration melting of moderately hydrous (1.7%–2.3% H_2O) medium- to high-K basaltic rocks can produce K-rich melts when SiO_2 >65 wt% (Sisson et al. 2005). Meanwhile, recent studies have suggested that a juvenile lower crust existed under central Tibet, characterized by positive zircon εHf(t) values and young crustal model ages (e.g., Zhu et al. 2011; Sui et al. 2013; Wu et al. 2015*a*). Liu et al. (2017) presented zircon Hf isotope data from the Dongqiao magmatic rocks, which are dominated by positive zircon εHf(t) values (−1.3 to + 8.2), indicating that a juvenile lower crust also existed in the Dongqiao area. Therefore, I-type granites from the Dongqiao area are inferred to have originated from a juvenile medium- to high-K mafic lower crust.

Furthermore, variations in SiO_2 content may result from the fractional crystallization of minerals. For example, the clear negative Ba, Sr, and Eu anomalies can be related to the fractionation of plagioclase and/or K-feldspar. Meanwhile, the relatively high K_2O content indicated that the main residual mineral in the source was plagioclase (fig. 4*c*). Moreover, the strong depletion in Nb, Ta, and Ti (fig. 5*a*, 5*b*) suggests the separation of rutile and/or ilmenite. In summary, I-type granites of the Dongqiao area were generated by partial melting of the juvenile mafic lower crust, followed by varying degrees of fractional crystallization.

A-Type Granites. A- and I-type granites of similar age coexist in the Dongqiao area. All of the samples have similar geochemical characteristics and evolutionary trends in whole-rock major and trace elements. Hu et al. (2017) reported geochemical and isotopic data for granodiorites from the Dongqiao area, which have positive zircon εHf(t) values (+0.9 to +6.8) and generally show a geochemical affinity with A-type granites. These similarities in geological, geochemical, and zircon-Hf isotopic characteristics lead us to propose that the A-type granites of this study were derived from the same source as the I-type granites, from juvenile mafic crust.

Creaser et al. (1991) proposed that A-type granites were generated by partial melting of an undepleted I-type tonalitic-granodioritic source. Moreover, experimental studies indicate that high-temperature and low-pressure (900°C, 4 kbar) dehydration melting of calc-alkaline granitoids in the middle crust (at depths of ≤15 km) would generate A-type magma (Skjerlie and Johnston 1993; Patiño Douce 1997). Accordingly, the widely distributed I-type calc-alkaline granitoids of central Tibet may provide a suitable protolith for the A-type granites, as supported by their depletion in some elements (e.g., Sr, Ba, Nb, Ta, and Ti; fig. 5*d*) that was possibly related to fractional crystallization of plagioclase, rutile, and ilmenite.

In summary, we propose that both I- and A-type granites were generated from juvenile mafic crust but at different depths. I-type granites were presumably formed by partial melting of a mafic lower-crustal source, while A-type granites were derived from a middle-crustal source, followed by crystal fractionation.

Tectonic Significance

Tectonic Setting. Diverse views exist on the timing of closure of the Bangong-Nujiang Ocean, although evidence increasingly suggests that closure was related to collision between the Lhasa and Qiangtang terranes in the early Early Cretaceous (Yin and Harrison 2000; Kapp et al. 2007; Zhu et al. 2009, 2011, 2013; Pan et al. 2012). As mentioned above, parts of the samples show the geochemical affinity with the typical A-type granites. Generally, A-type granites

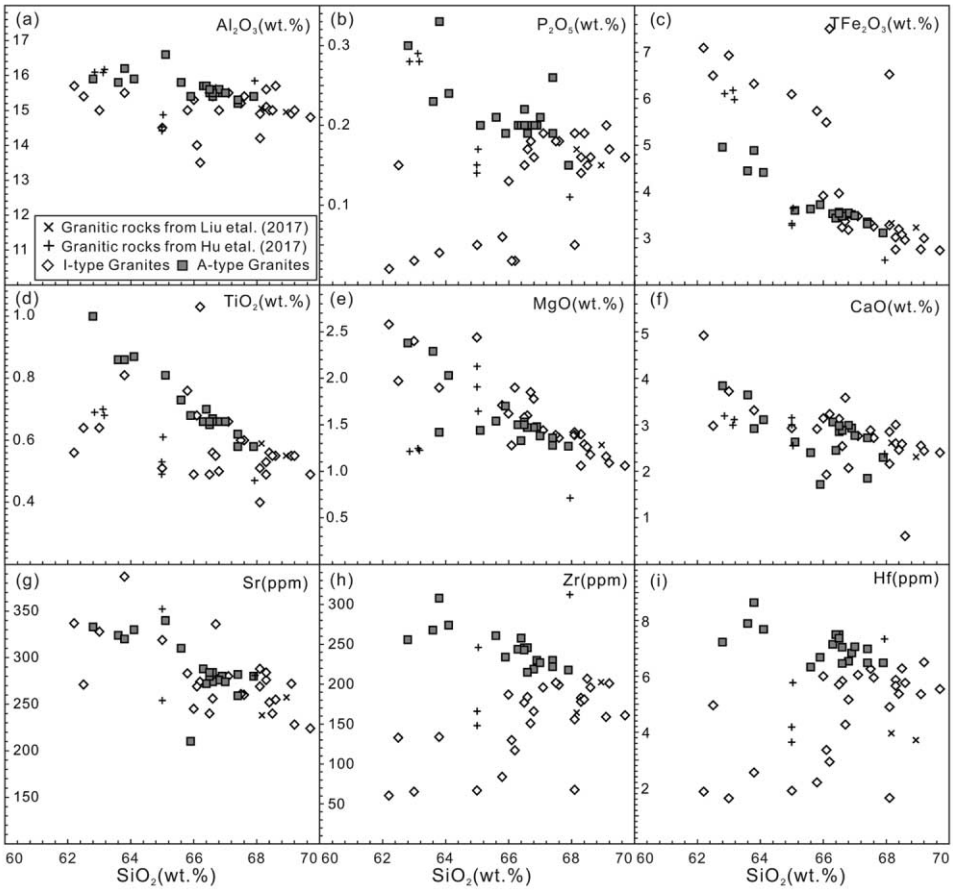

Figure 6. Whole-rock composition variation (Harker) diagrams of selected major and trace elements for the Dongqiao granitic rocks.

represent specific tectonic environments and can be divided into two types: A1-type, generally formed in a within-plate setting, and A2-type, formed during the postcollisional stage of orogenesis (Eby 1992; Bonin 2007). However, previous studies have found no clear boundary between A1- and A2-type granites (Eby 1990, 1992), finding instead that variations in their chemistry define a continuous spectrum. A-type rocks from the Dongqiao area plot at the junction between the fields of A1- and A2-type rocks on the discrimination diagrams (fig. 9*a*, 9*b*). Previous studies have reported the presence of coeval A2-type rocks (116–110 Ma) in the central and northern Lhasa terranes (Qu et al. 2012; Chen et al. 2014), indicating that coeval Early Cretaceous magmatic rocks in central Tibet formed during the postcollisional stage of orogenesis (Whalen et al. 1987; Eby 1992; Bonin 2007). This view is consistent with the samples plotting within the postcollisional granite field in Rb versus (Y + Nb) (fig. 9*c*; Pearce 1996) and Hf versus (Rb/30) versus (3Ta) (fig. 9*d*; Harris et al. 1986) discrimination diagrams. Therefore, we suggest that the Early Cretaceous magmatic flare-up (115–110 Ma) in the Dongqiao area occurred in a postcollision environment.

Geodynamic Model. It is generally considered that continental crust cannot reach temperatures high enough for dehydration melting without additional heat from the mantle (Thompson 2000). The generation of A-type magma is understood to require a high melting temperature (Clemens et al. 1986). Therefore, the widespread Early Cretaceous magma and A-type granites in central Tibet were probably associated with broad thermal anomalies linked to important geodynamic processes during the evolution of the BNSZ. The necessary mantle heat was possibly produced by upwelling of the asthenosphere or the emplacement of mantle-derived mafic magma. These developments could have arisen from various tectonic processes, such as slab breakoff or the delamination of thickened lithosphere (Whalen et al. 1996).

However, geodynamic mechanisms that controlled Early Cretaceous magmatic activity in central Tibet remain the subject of intense debate (e.g., Zhu et al. 2011, 2016; Wu et al. 2015*a*, 2015*b*;

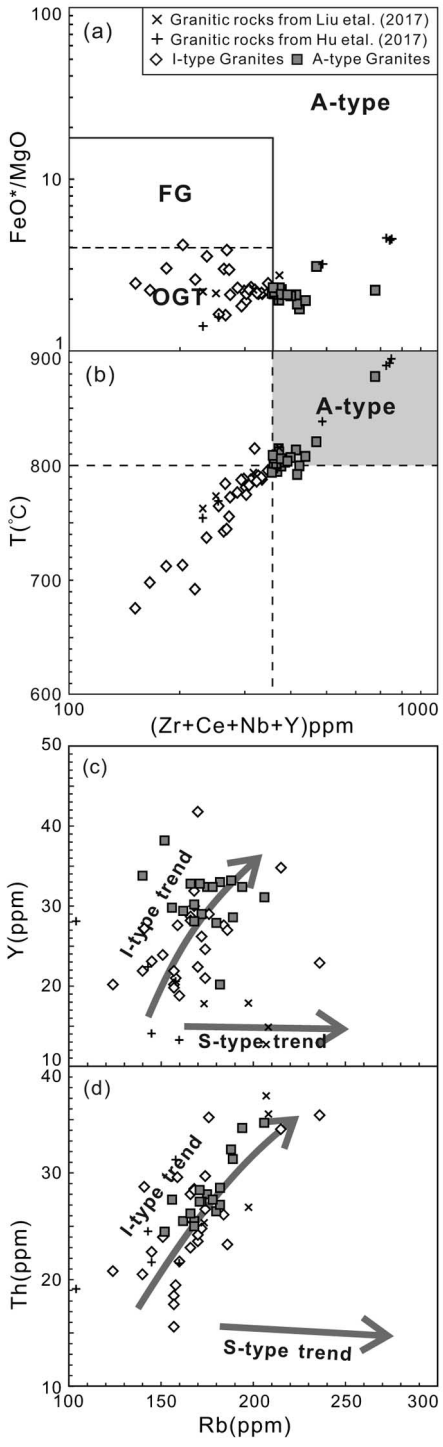

Figure 7. Geochemical classification diagrams for the Dongqiao granitic rocks. *a*, $(Na_2O + K_2O)/CaO$ versus (Zr + Nb + Ce + Y) (Whalen et al. 1987). *b*, Temperature (T; °C) versus (Zr + Nb + Ce + Y). *c*, Y versus Rb. *d*, Th versus Rb (Li et al. 2007). Abbreviations: FG = fractionated felsic granites; OGT = unfractionated I-, S-, and M-type granites.

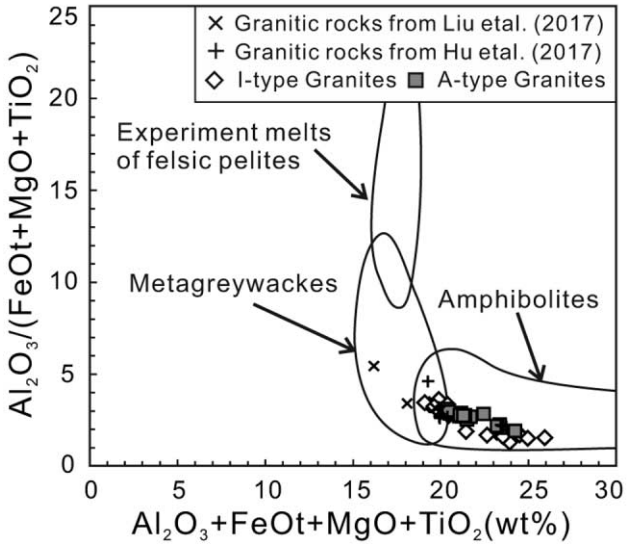

Figure 8. Geochemical classification diagrams for the Dongqiao granitic rocks: $Al_2O_3/(FeO_t + MgO + TiO_2)$ versus $(Al_2O_3 + FeO_t + MgO + TiO_2)$ (Patiño Douce 1999).

Xu et al. 2017). Recent new geological, geochronological, and geochemical data indicate that the Bangong-Nujiang ocean crust was consumed by divergent double subduction (e.g., Du et al. 2011; Wu et al. 2016*b*; Liu et al. 2017). Taking the Jurassic divergent double subduction into account, a new dynamic model comprising detaching and subsequent sinking of oceanic lithosphere due to gravitational instability has been proposed to explain the magmatic flare-up across central Tibet (Zhu et al. 2016). At present, we believe that this tectonic model may be the most reasonable explanation for the Early Cretaceous magmatism in the Dongqiao area (115–110 Ma)

During divergent double subduction and subsequent continent-continent collision between the Lhasa and Qiangtang terranes, slab rollback occurred, and the following mantle flow caused retreat of the hinge, finally resulting in detaching and sinking of the stagnant slab due to gravitational instability. The detaching and sinking of the ocean lithosphere provided the conditions for upwelling of the hot asthenosphere, resulting in a thermal anomaly and subsequent partial melting of the overriding plate. In summary, we suggest that such processes are likely to have caused the melting of mafic lower crust to generate I-type granites and of middle crust to generate A-type granites.

Conclusions

We have presented new data relating to the geochronology and geochemistry of the Dongqiao area, which,

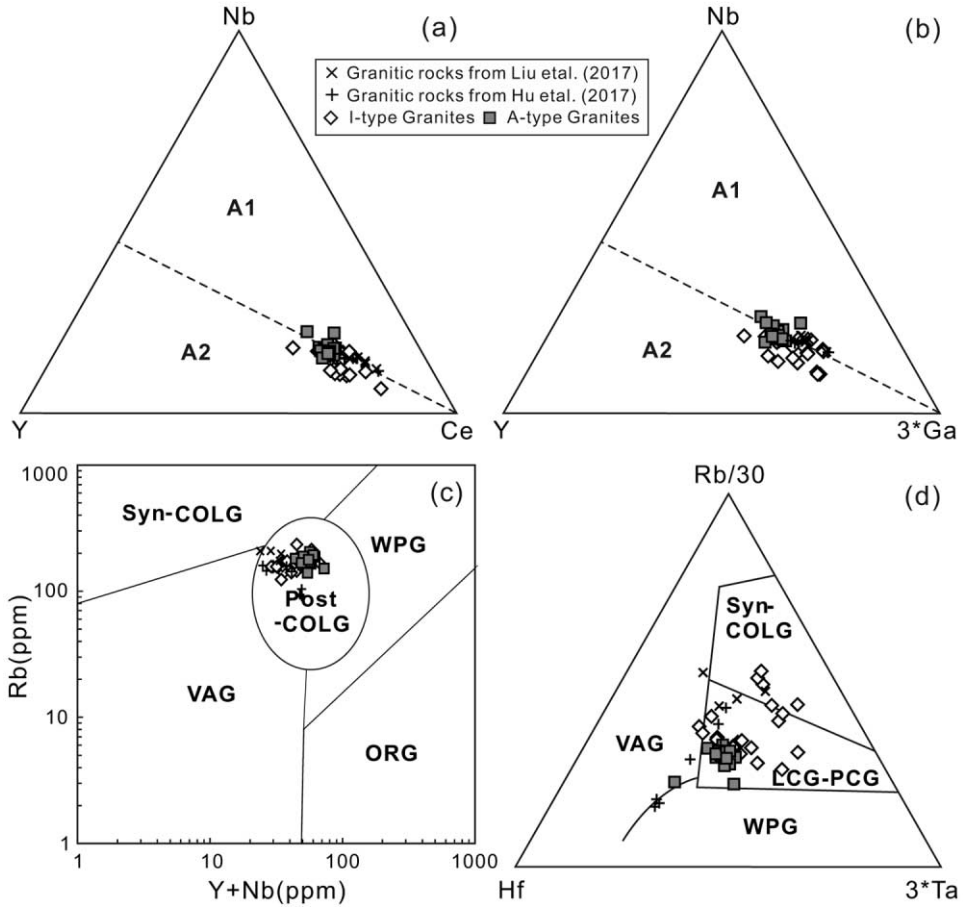

Figure 9. Geochemical classification diagrams for the Dongqiao granitic rocks. *a*, Nb-Y-Ce. *b*, Nb-Y-3*Ga (Eby 1992). *c*, Rb versus Y + Nb (Pearce 1996). *d*, Rb/30-Hf-Ta*3 (Harris et al. 1986). Abbreviations: VAG = volcanic arc granites; ORG = ocean ridge granites; WPG = within-plate granites; syn-COLG = syncollisional granites; post-COLG = postcollisional granites; LCG-PCG = late- and postcollisional granites.

together with data from previous studies, have led to the following conclusions.

1. New zircon U-Pb data indicate that large volumes of felsic magma were emplaced synchronously at 115–110 Ma in the Dongqiao area.

2. Geochemically, granitic rocks in the study area are divided into I- and A-type granites, which were formed by partial melting of juvenile crustal sources at different depths, following by varying degrees of fractional crystallization.

3. We consider the Early Cretaceous magma to have formed through postcollisional magmatism associated with the detachment and sinking of the Bangong-Nujiang oceanic lithosphere. During this process, upwelling of the asthenospheric mantle caused regional extension and provided a thermal anomaly that, in turn, caused subsequent partial melting of the overriding plate.

ACKNOWLEDGMENTS

This research was funded by the China Postdoctoral Science Foundation (2016M600353 and 2017T100321), the Fundamental Research Funds for the Central Universities (2017B11614), the Natural Science Foundation of Jiangsu Province (grants BK20170877), and the research grant of the State Key Laboratory of Isotope Geochemistry, Guangzhou Institute of Geochemistry, Chinese Academy of Sciences (SKLabIG-KF-16-11). Supporting data are included as tables S1 and S2.

Appendix
Descriptions of Analytical Methods

Laser Ablation Inductively Coupled Plasma Mass Spectrometry (LA-ICP-MS) Zircon U-Pb Dating. Zircon U-Pb dating and trace elements were analyzed using the LA-ICP-

MS system in the State Key Laboratory of Isotope Geochemistry, Guangzhou Institute of Geochemistry, Chinese Academy of Sciences. In this study, an Agilent 7500a ICP-MS coupled with a Resonetics RESOlution M-50 laser ablation system was used to analyze the U-Pb and trace elements of the zircons. The operating conditions for the laser ablation system, the ICP-MS instrument, and the data reduction methods are identical to those described by Hu et al. (2015).

Whole-Rock Geochemical Analysis. Whole-rock major and trace element analyses of the samples from the Dongqiao area were determined at the Sichuan Institute of Metallurgical Geology and Exploration, Chengdu, China. The major elemental compositions were analyzed using X-ray fluorescence spectrometry, and the trace element analyses were performed using an Agilent-7500a ICP-MS. Detailed operating conditions and data reduction are described by Huang et al. (2011).

REFERENCES CITED

Bonin, B. 2007. A-type granites and related rocks: evolution of a concept, problems and prospects. Lithos 97: 1–29.

Chang, Q. S. 2012. Petrology, geochronology and geochemistry of Rena-Co volcanic rocks along southern margin of Qiangtang Terrane, Tibetan Plateau. PhD dissertation, China University of Geosciences (in Chinese with English abstract).

Chappell, B. W. 1999. Aluminium saturation in I- and S-type granites and the characterization of fractionated haplogranites. Lithos 46:535–551.

Chappell, B. W., and White, A. J. R. 1974. Two contrasting granite types. Pacific Geology 8:173–174.

Chen, Y.; Zhu, D. C.; Zhao, Z. D.; Meng, F. Y.; Wang, Q.; Santosh, M.; Dong, G. C.; and Mo, X. X. 2014. Slab breakoff triggered ca. 113 Ma magmatism around Xainza area of the Lhasa Terrane, Tibet. Gondwana Res. 26:449–463.

Chung, S. L.; Chu, M. F.; Zhang, Y. Q.; Xie, Y. W.; Lo, C. H.; Lee, T. Y.; Lan, C. Y.; Li, X. H.; Zhang, Q.; and Wang, Y. Z. 2005. Tibetan tectonic evolution inferred from spatial and temporal variations in post-collisional magmatism. Earth-Sci. Rev. 68:173–196.

Clemens, J. D.; Holloway, J. R.; and White, A. R. J. 1986. Origin of A-type granite: experimental constraints. Am. Mineral. 79:71–86.

Creaser, R. A.; Price, R. C.; and Wormold, R. J. 1991. A-type granite revised: assessment of residual source model. Geology 19:163–166.

Dewey, J. F.; Shackleton, R. M.; Chang, C. F.; and Sun, Y. Y. 1988. The tectonic evolution of the Tibetan Plateau. Philos. Trans R. Soc. A 327:379–413.

Ding, L.; Kapp, P.; Zhong, D. L.; and Deng, W. M. 2003. Cenozoic volcanism in Tibet: evidence for a transition from oceanic to continental subduction. J. Petrol. 44: 1833–1865.

Du, D. D.; Qu, X. M.; Wang, G. H.; Xin, H. B.; and Liu, Z. B. 2011. Bidirectional subduction of the Middle Tethys oceanic basin in the west segment of Bangonghu-Nujiang suture, Tibet: evidence from zircon U-Pb LA-ICP-MS dating and petrogeochemistry of arc granites. Acta Petrol. Sin. 27:1993–2002 (in Chinese with English abstract).

Eby, G. N. 1990. The A-type granitoids: a review of their occurrence and chemical characteristics and speculations on their petrogenesis. Lithos 26:115−134.

———. 1992. Chemical subdivision of the A-type granitoids: petrogenetic and tectonic implications. Geology 20:641– 644.

Harris, N. B. W.; Pearce, J. A.; and Tindle, A. G. 1986. Geochemical characteristics of collision-zone magmatism. Geol. Soc. Lond. Spec. Publ. 19:67–81.

Hastie, A. R.; Kerr, A. C.; Pearce, J. A.; and Mitchell, S. F. 2007. Classification of altered volcanic island arc rocks using immobile trace elements: development of the Th–Co discrimination diagram. J. Petrol. 48:2341–2357.

Hu, P. Y.; Zhai, Q. G.; Jahn, B. M.; Wang, J.; Li, C.; Chung, S. L.; Lee, H. Y.; and Tang, S. H. 2017. Late Early Cretaceous magmatic rocks (118–113 Ma) in the middle segment of the Bangong–Nujiang suture zone, Tibetan Plateau: evidence of lithospheric delamination. Gondwana Res. 44:116–138.

Hu, Y. B.; Liu, J. Q.; Ling, M. X.; Ding, W.; Liu, Y.; Zartman, R. E.; Ma, X. F.; et al. 2015. The formation of qulong adakites and their relationship with porphyry copper deposit: geochemical constraints. Lithos 220:60–80.

Huang, Y.; Tang, J. X.; Lang, X. H.; Zhang, L.; and Chen, Y. 2011. Geochemical characteristics of intrusive and volcanic rocks in No. II ore body of Xiongcun copper-gold deposit, Tibet: constraints on rock genesis and tectonic setting. Miner. Depos. 30:0361–0373 (in Chinese with English abstract).

Kang, Z. Q.; Xu, J. F.; Dong, Y. H.; and Wang, B. Q. 2008. Cretaceous volcanic rocks of Zenong Group in north-middle Lhasa Block: products of southward subducting of the Slainajap ocean? Acta Petrol. Sin. 24:303–314 (in Chinese with English abstract).

Kang, Z. Q.; Xu, J. F.; Wang, B. D.; Dong, Y. H.; Wang, S. Q.; and Chen, J. L. 2009. Geochemistry of Cretaceous volcanic rocks of Duoni Formation in Northern Lhasa Block: discussion of tectonic setting. Earth Sci. J. China Univ. Geosci. 34:89–104 (in Chinese with English abstract).

Kapp, P.; DeCelles, P. G.; Gehrels, G. E.; Heizler, M.; and Ding, L. 2007. Geological records of the Lhasa-Qiangtang and Indo-Asian collisions in the Nima area of central Tibet. Geol. Soc. Am. Bull. 119:917–932.

Kapp, P.; Yin, A.; Harrison, T. M.; and Ding, L. 2005. Cretaceous-Tertiary shortening, basin development, and volcanism in central Tibet. Geol. Soc. Am. Bull. 117: 865–878.

Leier, A. L.; Decelles, P. G.; Kapp, P.; and Gehrels, G. E. 2007*a*. Lower Cretaceous strata in the Lhasa Terrane,

Tibet, with implications for understanding the early tectonic history of the Tibetan Plateau. J. Sediment. Res. 77:809–825.

Leier, A. L.; Kapp, P.; Gehrels, G. E.; and DeCelles, P. G. 2007*b*. Detrital zircon geochronology of Carboniferous–Cretaceous strata in the Lhasa Terrane, Southern Tibet. Basin Res. 19:361–378.

Le Maitre, R. W.; Bateman, P.; Dudek, A.; Keller, J.; Lameyre, J.; Le Bas, M. J.; Sabine, P. A.; et al. 1989. A classification of igneous rocks and a glossary of terms. Oxford, Blackwell.

Li, X. H.; Li, Z. X.; Li, W. X.; Liu, Y.; Yuan, C.; Wei, G. J.; and Qi, C. S. 2007. U–Pb zircon, geochemical and Sr–Nd–Hf isotopic constraints on age and origin of Jurassic I- and A-type granites from central Guangdong, SE China: a major igneous event in response to foundering of a subducted flat-slab? Lithos 96:186–204.

Liu, D. L.; Shi, R. D.; Ding, L.; Huang, Q. S.; Zhang, X. R.; Yue, Y. H.; and Zhang, L. Y. 2017. Zircon U–Pb age and Hf isotopic compositions of Mesozoic granitoids in southern Qiangtang, Tibet: implications for the subduction of the Bangong–Nujiang Tethyan Ocean. Gondwana Res. 41:157–172.

Liu, T.; Zhai, Q. G.; Wang, J.; Bao, P. S.; Qiangba, Z.; Tang, S. H.; and Tang, Y. 2015. Tectonic significance of the Dongqiao ophiolite in the north-central Tibetan plateau: evidence from zircon dating, petrological, geochemical and Sr–Nd–Hf isotopic characterization. J. Asian Earth Sci. 116:139–154.

Lustrino, M. 2005. How the delamination and detachment of lower crust can influence basaltic magmatism. Earth-Sci. Rev. 72:21–38.

Maniar, P. D., and Piccoli, P. M. 1989. Tectonic discrimination of granitoids. Geol. Soc. Am. Bull. 101:635–643.

Middlemost, E. A. K. 1994. Naming materials in the magma/igneous rock system. Earth-Sci. Rev. 74:193–227.

Pan, G. T.; Wang, L. Q.; Li, R. S.; Yuan, S. H.; Ji, W. H.; Yin, F. G.; Zhang, W. P.; and Wang, B. D. 2012. Tectonic evolution of the Qinghai-Tibet plateau. J. Asian Earth Sci. 53:3–14.

Patiño Douce, A. E. 1997. Generation of metaluminous A-type granites by low-pressure melting of calc-alkaline granitoids. Geology 25:743–746.

———. 1999. What do experiments tell us about the relative contributions of crust and mantle to the origin of granitic magmas? Geol. Soc. Lond. Spec. Publ. 168:55–75.

Pearce, J. A. 1996. Sources and settings of granitic rocks. Episodes 19:120–125.

Petford, N., and Atherton, M. 1996. Na-rich partial melts from newly underplated basaltic crust: the Cordillera Blanca Batholith, Peru. J. Petrol. 37:1491–1521.

Qiangba, Z. X.; Wu, H.; Gesang, W. D.; Ciren, O. Z.; Basang, D. Z.; Qiong, D.; and Nv, D. W. 2016. Early Cretaceous magmatism in Dongqiao, Tibet: implications for the evolution of the Bangong–Nujiang Ocean and crustal growth in a continent–continent collision zone. Geol. Bull. China 35:648–666 (in Chinese with English abstract).

Qu, X. M.; Wang, R. J.; Xin, H. B.; Jiang, J. H.; and Chen, H. 2012. Age and petrogenesis of A-type granites in the middle segment of the Bangonghu–Nujiang suture, Tibetan plateau. Lithos 146/147:264–275.

Rapp, R. P., and Watson, E. B. 1995. Dehydration melting of metabasalt at 8–32 kbar: implications for continental growth and crust-mantle recycling. J. Petrol. 36:891–931.

Rickwood, P. C. 1989. Boundary lines within petrologic diagrams which use oxides of major and minor elements. Lithos 22:247–263.

Rushmer, T. 1991. Partial melting of two amphibolites: contrasting experimental results under fluid-absent conditions. Contrib. Mineral. Petrol. 107:41–59.

Shand, S. J. 1943. Eruptive rocks: their genesis, composition, classification, and their relation to ore-deposits with a chapter on meteorite. New York, Wiley.

Sisson, T. W.; Ratajeski, K.; Hankins, W. B.; and Glazner, A. F. 2005. Voluminous granitic magmas from common basaltic sources. Contrib. Mineral. Petrol. 148: 635–661.

Skjerlie, K. P., and Johnston, A. D. 1993. Vapor-absent melting at 10 kbar of biotite- and amphibole-bearing tonalitic gneiss: implications for the generation of A-type granites. Geology 20:263–266.

Sui, Q. L.; Wang, Q.; Zhu, D. C.; Zhao, Z. D.; Chen, Y.; Santosh, M.; Hu, Z. C.; Yuan, H. L.; and Mo, X. X. 2013. Compositional diversity of ca. 110 Ma magmatism in the northern Lhasa Terrane, Tibet: implications for the magmatic origin and crustal growth in a continent–continent collision zone. Lithos 168/169:144–159.

Sun, S. S., and McDonough, W. F. 1989. Chemical and isotope systematics of oceanic basalts: implications for mantle composition and processes. *In* Saunders, A. D., and Norry, M. J., eds. Magmatism in the ocean basins. Geol. Soc. Spec. Publ. 42:313–345.

Thompson, A. B. 2000. Some space-time relationship for crustal melting and granitic intrusion at various depths. *In* Castro, A.; Fernandez, C.; and Vigneresse, J. L., eds. Understanding granites: integrating new and classic techniques. Geol. Soc. Lond. Spec. Publ. 168:7–25.

Watson, E. B.; Wark, D. A.; and Thomas, J. B. 2006. Crystallization thermometers for zircon and rutile. Contrib. Mineral. Petrol. 151:413–433.

Whalen, J. B.; Currie, K. L.; and Chappell, B. W. 1987. A-type granites: geochemical characteristics, discrimination and petrogenesis. Contrib. Mineral. Petrol. 95: 407–419.

Whalen, J. B.; Jenner, G. A.; Longstaffe, F. J.; Robert, F.; and Gariepy, C. 1996. Geochemical and isotopic (O, Nd, Pb and Sr) constraints on A-type granite: petrogenesis based on the Topsails igneous suite, Newfoundland Appalachians. J. Petrol. 37:1463–1489.

Wu, H.; Li, C.; Chen, J. W.; and Xie, C. M. 2016*a*. Late Triassic tectonic framework and evolution of Central Qiangtang, Tibet, SW China. Lithosphere 8:141–149.

Wu, H.; Li, C.; Hu, P. Y.; and Li, X. K. 2015*b*. Early cretaceous (100–105 Ma) adakitic magmatism in the Dachagou area, northern Lhasa terrane, Tibet: implications for the Bangong-Nujiang Ocean subduction and slab break-off. Int. Geol. Rev. 57:1172–1188.

Wu, H.; Li, C.; Xu, M. J.; and Li, X. K. 2015*a*. Early cretaceous adakitic magmatism in the Dachagou area,

northern Lhasa terrane, Tibet: implications for slab rollback and subsequent slab break-off of the lithosphere of the Bangong–Nujiang Ocean. J. Asian Earth Sci. 97: 51–66.

Wu, H.; Xie, C. M.; Li, C.; Wang, M.; Fan, J. J.; and Xu, W. 2016*b*. Tectonic shortening and crustal thickening in subduction zones: evidence from Middle–Late Jurassic magmatism in Southern Qiangtang, China. Gondwana Res. 39:1–13.

Xu, W.; Li, C.; Wang, M.; Fan, J. J.; Wu, H.; and Li, X. 2017. Subduction of a spreading ridge within the Bangong Co–Nujiang Tethys Ocean: evidence from Early Cretaceous mafic dykes in the Duolong porphyry Cu–Au deposit, western Tibet. Gondwana Res. 41:128–141.

Yin, A., and Harrison, T. M. 2000. Geologic evolution of the Himalayan-Tibetan orogen. Annu. Rev. Earth Planet. Sci. 28:211–280.

Zhang, L. L.; Zhu, D. C.; Zhao, Z. D.; Liao, Z. L.; Wang, L. Q.; and Mo, X. X. 2011. Early granitoids in Xainza, Tibet: evidence of slab break-off. Acta Petrol. Sin. 27: 1938–1948 (in Chinese with English abstract).

Zhu, D. C.; Li, S. M.; Cawood, P. A.; Wang, Q.; Zhao, Z. D.; Liu, S. A.; and Wang, L. Q. 2016. Assembly of the Lhasa and Qiangtang terranes in central Tibet by divergent double subduction. Lithos 245:7–17.

Zhu, D. C.; Mo, X. X.; Niu, Y.; Zhao, Z. D.; Wang, L. Q.; Liu, Y. S.; and Wu, F. Y. 2009. Geochemical investigation of Early Cretaceous igneous rocks along an east–west traverse throughout the central Lhasa Terrane, Tibet. Chem. Geol. 268:298–312.

Zhu, D. C.; Zhao, Z. D.; Niu, Y. L.; Dilek, Y.; Hou, Z. Q.; and Mo, X. X. 2013. The origin and pre-Cenozoic evolution of the Tibetan plateau. Gondwana Res. 23:1429–1454.

Zhu, D. C.; Zhao, Z. D.; Niu, Y.; Mo, X. X.; Chung, S. L.; and Hou, Z. Q. 2011. The Lhasa Terrane: record of a microcontinent and its histories of drift and growth. Earth Planet. Sci. Lett. 301:241–255.